SCIENCE CHINA
Information Sciences

• RESEARCH PAPER •

August 2026, Vol. 69, Iss. 8, 180505:1–180505:6
https://doi.org/10.1007/s11432-026-5008-4

Special Topic: Quantum Information

Deterministic distribution of Gaussian entanglement and quantum steering through fiber channels

Yanru YAN[1], Siyu REN[1], Mengyu ZHAO[1], Dongmei HAN[1], Yalin LI[1], Meihong WANG[1,2] & Xiaolong SU[1,2*]

[1]*State Key Laboratory of Quantum Optics Technologies and Devices, Institute of Opto-Electronics, Shanxi University, Taiyuan 030006, China*
[2]*Collaborative Innovation Center of Extreme Optics, Shanxi University, Taiyuan 030006, China*

Received 4 March 2026/Revised 27 April 2026/Accepted 17 June 2026/Published online 16 July 2026

Abstract Quantum entanglement and quantum steering, as important quantum resources, are of great significance in the field of quantum information science. Toward practical quantum communication, it is essential to distribute Gaussian entanglement and quantum steering through optical fiber channels. Here, we experimentally demonstrate the distribution of deterministic Einstein-Podolsky-Rosen (EPR) entanglement and EPR steering through fiber channels. By transmitting the EPR entangled light and the local oscillator (LO) over independent fiber channels, the excess noise in the quantum channel is reduced. Utilizing this transmission approach, we extend the transmission distance of continuous-variable (CV) entanglement distribution to 60.26 km and that of CV EPR steering to 10.06 km in fiber channels. Our results take a crucial step toward practical quantum communication with CV entanglement and quantum steering in fiber channels.

Keywords quantum entanglement, quantum steering, distribution, fiber channel, continuous-variable

Citation Yan Y R, Ren S Y, Zhao M Y, et al. Deterministic distribution of Gaussian entanglement and quantum steering through fiber channels. Sci China Inf Sci, 2026, 69(8): 180505, https://doi.org/10.1007/s11432-026-5008-4

1 Introduction

Gaussian entanglement and quantum steering are essential quantum resources that have pivotal importance in the fields of quantum computation [1–6], quantum communication [7–13], and quantum metrology [14–16]. Different from the verification of quantum entanglement with a trusted measurement device, quantum steering verification [17–19] is performed in a one-sided-device-independent (1SDI) scenario, where the measurement device on one side is untrusted [20–25]. It has been shown that one-way steering occurs in a certain asymmetric system [26–30]. Due to its unique feature, EPR steering can be potentially applied to 1SDI channel discrimination [31], secure quantum teleportation [32], quantum key distribution [22–25], and remote state preparation [33].

Distribution of quantum entanglement and quantum steering in quantum channels is the precondition for the entanglement-assisted or steering-assisted quantum communication [33–37]. Although the distribution distance of discrete-variable (DV) quantum entanglement has been extended to over hundreds of km in fiber channel, the transmission distance of continuous-variable (CV) quantum entanglement remains to dozens of km [38], and the distribution distance of CV quantum steering is around 2 km [11]. This is because the CV entanglement and steering not only decrease with loss, but also are affected by the excess noise introduced in the fiber channel. Most challenging, the sudden death of deterministic quantum entanglement and steering happens in a noisy environment [39]. Compared to probabilistic generation of DV entanglement, CV entanglement can be generated deterministically, which enables high-efficiency entanglement-based quantum communication. Thus, the extension of transmission distance for CV entanglement and steering in a fiber channel is essential.

Here, we experimentally demonstrate the distribution of Gaussian entanglement through a 60.26 km fiber channel and CV quantum steering over a 10.06 km fiber channel. The two EPR entangled modes at the central quantum server are transmitted to two users, Alice and Bob, through fiber channels, respectively. In order to reduce the excess noise introduced in the fiber channel, we transmit the local oscillator (LO) beam through another independent fiber channel. By measuring the received modes in the time domain at the users' stations with a homodyne detector,

* Corresponding author (email: suxl@sxu.edu.cn)

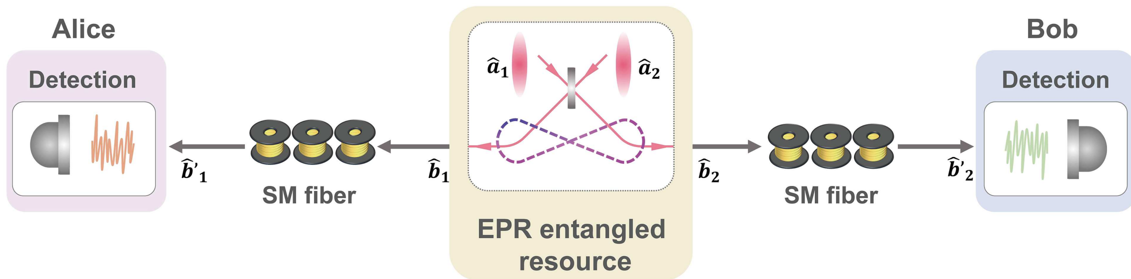

Figure 1 (Color online) The schematic of quantum entanglement and steering distribution through fiber channels. Quantum cloud server produces the EPR entanglement state and distributes the entangled modes to users (Alice and Bob) through single-mode fiber channels.

we reconstruct the covariance matrix of output states and quantify the distributed quantum entanglement and quantum steering at different transmission distances. We show that after transmission distances of 60.26 and 10.06 km, the quantum entanglement and steering still exist. Our results provide a reference for CV entanglement-based and steering-based quantum communication in a fiber channel.

2 The principle

As shown in Figure 1, a Gaussian EPR entangled state is generated by combining two amplitude-squeezed beams ($\hat{a}_1$ and $\hat{a}_2$) at a balanced beamsplitter on the central quantum server. The entangled modes ($\hat{b}_1$ and $\hat{b}_2$) are subsequently sent to two users (Alice and Bob) via fiber channels, respectively. The transmission distances in two independent fiber channels are the same, which guarantees the coherence of the distributed modes. Finally, Alice and Bob perform measurements on the distributed modes to verify the distributed quantum entanglement and steering.

The shared CV Gaussian entangled state between two users can be characterized by its covariance matrix, with elements defined as [40]

$$\sigma_{ij} = \frac{1}{2}\langle \hat{\xi}_i\hat{\xi}_j + \hat{\xi}_j\hat{\xi}_i\rangle - \langle\hat{\xi}_i\rangle\langle\hat{\xi}_j\rangle, \tag{1}$$

where $\hat{\boldsymbol{\xi}} \equiv (\hat{x}_1, \hat{p}_1, \hat{x}_2, \hat{p}_2)^{\mathrm{T}}$ is the vector containing the amplitude and phase quadratures for each mode, and $\hat{\xi}_{i(j)}$ is the $i(j)$-th element of the vector $\hat{\boldsymbol{\xi}}$. The quadrature operators are denoted by $\hat{x} = \hat{a}^\dagger + \hat{a}$, $\hat{p} = i(\hat{a}^\dagger - \hat{a})$, where $\hat{a}^\dagger$ and $\hat{a}$ are creation and annihilation operators, respectively. According to this definition, the covariance matrix of the EPR entangled state is given by

$$\boldsymbol{\sigma} = \begin{pmatrix} \mathbf{A} & \mathbf{C} \\ \mathbf{C}^{\mathrm{T}} & \mathbf{B} \end{pmatrix}, \tag{2}$$

where the submatrices $\mathbf{A} = \begin{bmatrix} V(\hat{x}_1) & 0 \\ 0 & V(\hat{p}_1) \end{bmatrix}$ and $\mathbf{B} = \begin{bmatrix} V(\hat{x}_2) & 0 \\ 0 & V(\hat{p}_2) \end{bmatrix}$ represent the two entangled modes respectively, $V(\hat{x}_i)$ ($V(\hat{p}_i)$) and T denote the variance of amplitude (phase) quadratures and transpose, and $\mathbf{C} = \begin{bmatrix} \sigma(\hat{x}_1, \hat{x}_2) & 0 \\ 0 & \sigma(\hat{p}_1, \hat{p}_2) \end{bmatrix}$ represents the covariance between two modes.

After transmission through a fiber channel, the distributed mode of the entangled state $\hat{b}'_i$ $(i = 1, 2)$ is given by $\hat{b}'_i = \sqrt{\eta_i}\hat{b}_i + \sqrt{1-\eta_i}(\hat{\nu}_i + \hat{N}_i)$. Here, η_i denotes the channel's transmission efficiency, while $\hat{\nu}_i$ and $\hat{N}_i$ represent the vacuum and excess noise introduced in the fiber channel, respectively. Besides the loss and noise introduced in the fiber channel, the phase fluctuations, which increase with transmission distance, are another parameter that affects the distributed entanglement and quantum steering. By substituting the expression of the distributed modes into the covariance matrix, the output covariance matrix through fiber channels can be obtained (see Appendix A for more details).

For a Gaussian entangled state, the positive partial transpose (PPT) criterion constitutes a sufficient and necessary condition [41]. The bipartite Gaussian states are entangled if and only if the minimum symplectic eigenvalue ν_- of the covariance matrix $\boldsymbol{\sigma}$ satisfies the inequality $\nu_- < 1$. For a two-mode Gaussian state, ν_- is determined by

$$\nu_- = \sqrt{\frac{\Delta - \sqrt{\Delta^2 - 4\zeta}}{2}}, \tag{3}$$

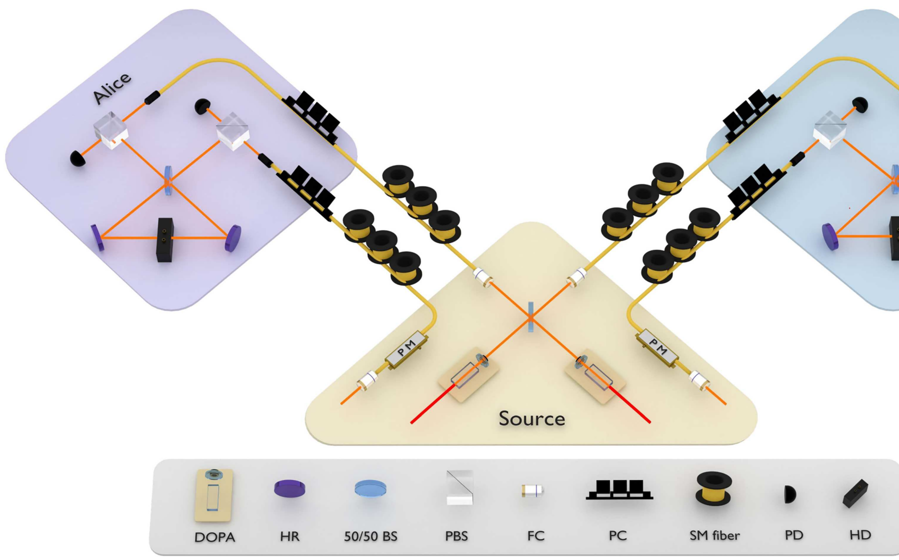

Figure 2 (Color online) The experimental setup of Gaussian entanglement and quantum steering distribution through fiber channels. Two degenerate optical parametric amplifiers (DOPA1 and DOPA2) each prepare a squeezed state possessing 6 dB squeezing and 10 dB anti-squeezing. The distributed modes of the EPR entangled state are measured by two balanced homodyne detectors. These measurements enable us to reconstruct part of the covariance matrix. The red lines in the figure represent light at 775 nm, and the orange lines represent light at 1550 nm.

where $\zeta = \det \boldsymbol{\sigma}$ and $\Delta = \det \mathbf{A} + \det \mathbf{B} + 2\det \mathbf{C}$. According to the covariance matrix $\boldsymbol{\sigma}$, EPR steering between Alice and Bob for CV Gaussian states can be quantified as [42]

$$\begin{aligned} \mathcal{G}^{A\to B} &= \max\left\{0, \frac{1}{2}\ln\frac{\det \mathbf{A}}{\det \boldsymbol{\sigma}}\right\}, \\ \mathcal{G}^{B\to A} &= \max\left\{0, \frac{1}{2}\ln\frac{\det \mathbf{B}}{\det \boldsymbol{\sigma}}\right\}, \end{aligned} \tag{4}$$

when $\mathcal{G}^{A\to B} > 0$, Alice is capable of steering Bob's state. Correspondingly, $\mathcal{G}^{B\to A} > 0$ implies that Bob can steer Alice.

3 The experiment

As illustrated in Figure 2, two amplitude-squeezed states are produced by two degenerate optical parametric amplifiers (DOPAs) operated below the threshold, respectively. By combining two squeezed modes at a balanced beamsplitter with their relative phase locked at $\pi/2$, a CV EPR entangled state of amplitude-anti-correlation and phase-correlation is generated. The two modes of the EPR state are coupled into two single-mode fibers (Corning SMF-28 ultra) and distributed to Alice and Bob, respectively, with the fiber coupling efficiency of 95%.

To reduce the excess noise in the fiber channel carrying the EPR state, we distribute the LO beam through an independent fiber channel to Alice and Bob. In this case, the excess noise is significantly lower than that of conventional polarization multiplexing schemes. After receiving the transmitted modes, Alice and Bob employ balanced homodyne detectors to measure the amplitude and phase quadratures of received EPR lights. The interference efficiency at every beamsplitter is measured to be 99%. By refining the phase locking system, the phase fluctuations after propagation through the fiber channels are reduced to 1.15° to 3.51° with the transmission distance of 0.008 to 30.13 km (Table 1, see Appendix B for more details).

Alice and Bob perform time domain measurements on the distributed modes simultaneously and respectively. In the measurement, the output signals of the two homodyne detectors are extracted with a sideband frequency of 9 MHz and a filter bandwidth of 30 kHz. At a sampling rate of 1 MS/s, the demodulated signals are captured in parallel by an oscilloscope with digital storage capability. By changing the relative phase difference of the users' homodyne detectors, the quadratures (amplitude and phase) of distributed modes are measured.

Table 1 The experimental parameters at different fiber transmission distances.

Distance (km)	Channel efficiency (η_1)	Channel efficiency (η_2)	Excess noise	Phase fluctuation (°)
0.008	0.93	0.94	0.007	1.15
1.95	0.85	0.86	0.010	1.58
5.03	0.74	0.74	0.011	1.69
10.05	0.58	0.58	0.013	2.65
20.09	0.37	0.37	0.016	3.21
30.13	0.23	0.23	0.020	3.51

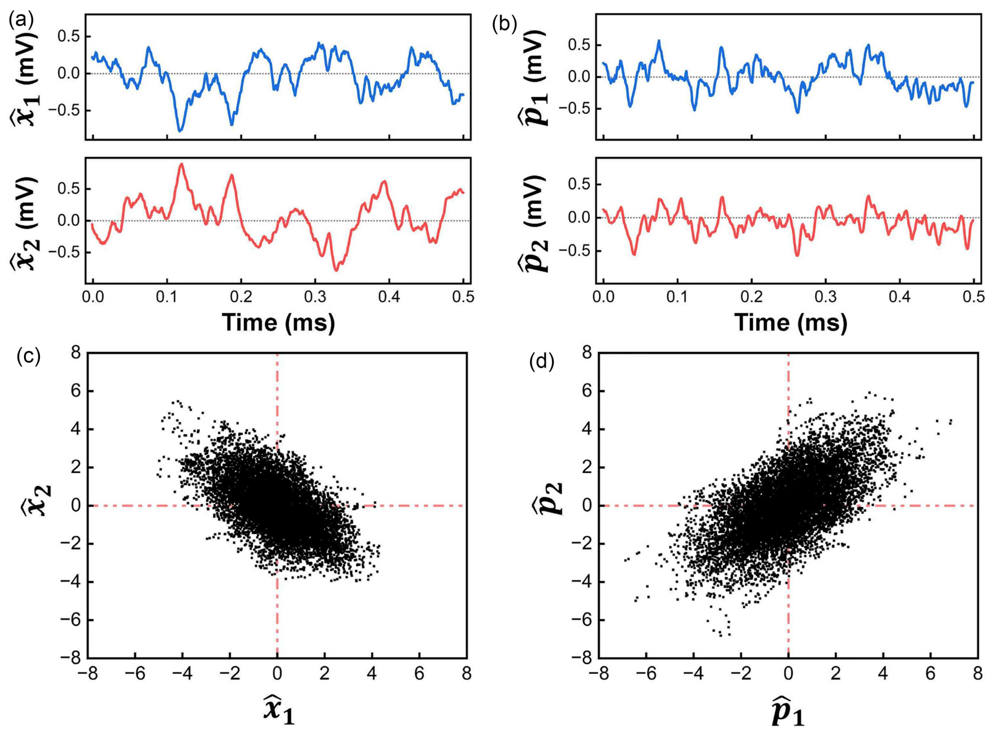

Figure 3 (Color online) Results for entanglement distribution over 60.26 km transmission distance. (a) and (b) show the corresponding AC signals obtained via homodyne detection, with 500 data points presented in each. (c) and (d) display the correlations of the two users' data, each containing 10000 experimental data points. Here, $\hat{x}_1$ and $\hat{x}_2$ ($\hat{p}_1$ and $\hat{p}_2$) denote the amplitude (phase) quadratures of the entangled state.

4 Results

We perform entanglement distribution experiments at transmission distances of 0.016, 3.90, 10.06, 20.10, 40.18, and 60.26 km. Figures 3(a) and (b) display the observed amplitude and phase quadratures in the time domain of two distributed modes at two users' stations after transmission of 60.26 km. It is obvious that the correlation exists in the amplitude and phase quadratures of the two distributed modes. We also plot the anti-correlation (correlation) in the amplitude (phase) quadrature of the two distributed modes after a 60.26 km single-mode optical fiber, as shown in Figures 3(c) and (d). This confirms that the quantum correlation of the EPR entangled state exists after the transmission through 60.26 km fiber channels.

Based on the measured amplitude and phase quadratures of two distributed modes, we reconstruct the covariance matrix of the distributed state at different transmission distances (see Appendix C for more details). Then we quantify the distributed entanglement and quantum steering according to (3) and (4), respectively. The relevant experimental parameters are summarised in Table 1, where the transmission distances from source to Alice (Bob) are presented, and the total transmission distances are double those distances. The channel efficiency decreases as transmission distances increase, while excess noise and phase fluctuation increase with the transmission distances.

The average PPT values of the distributed state are 0.29, 0.35, 0.44, 0.55, 0.72, and 0.82 at the corresponding transmission distances, as represented by the red data points in Figure 4(a). Furthermore, the theoretical prediction (blue curve in Figure 4(a)) depicts the PPT values for EPR beams transmitted through the single-mode fiber, matching well with the experimental data. Entanglement remains observable over a transmission distance of more than 60.26 km. The PPT values increase gradually with transmission distance, which means that the distributed

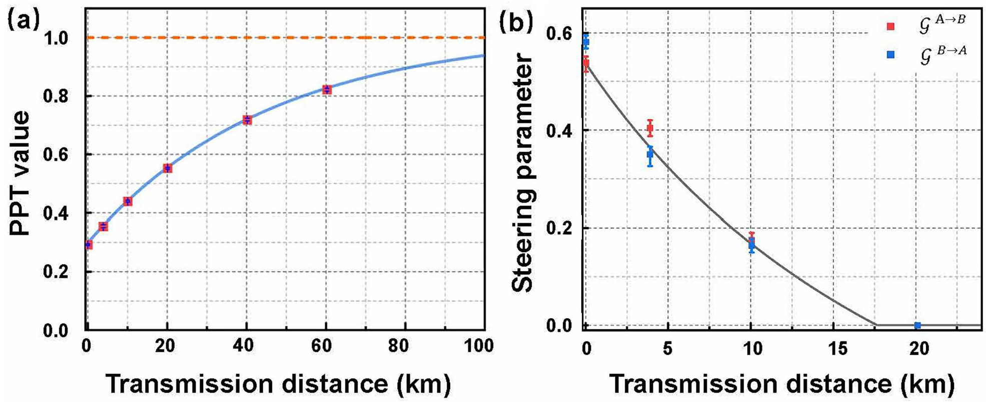

Figure 4 (Color online) Experimental results. (a) The experimental results (red solid squares) for the minimum symplectic eigenvalues (PPT values) of the EPR entangled light closely match the theoretical prediction (blue solid curve) across the transmission distance; (b) the steerability $\mathcal{G}^{A\to B}$ (Alice to Bob, red solid squares) and $\mathcal{G}^{B\to A}$ (Bob to Alice, blue solid squares) are measured at transmission distances of 0.016, 3.90, and 10.06 km. The gray curve represents the theoretical prediction for both $\mathcal{G}^{A\to B}$ and $\mathcal{G}^{B\to A}$, which are fully overlapped. The error bars are derived from ten datasets.

entanglement decreases gradually as transmission distance increases.

In Figure 4(b), the Gaussian steerability $\mathcal{G}^{A\to B}$ ($\mathcal{G}^{B\to A}$) is measured as 0.54 (0.58) at 0.016 km, 0.40 (0.35) at 3.90 km, and 0.18 (0.16) at 10.06 km. The gray curve represents the theoretical prediction of the steerability depending on transmission distance, which matches well with the experimental data. Clearly, the Gaussian steerabilities decrease as transmission distance increases, vanishing beyond 17.5 km. Small differences are observed for the steerabilities $\mathcal{G}^{A\to B}$ and $\mathcal{G}^{B\to A}$ in transmission distances of 0.016 and 3.90 km, since the criterion of Gaussian steerability is more sensitive to the imperfection of elements in the covariance matrix than that of Gaussian entanglement.

According to the experimental results shown in Figures 4(a) and (b), as the transmission distance increases, quantum steering disappears before entanglement does. This occurs because, in the quantum correlation hierarchy, quantum steering is a stricter correlation than entanglement; when there is steering, there must be entanglement, but entanglement does not guarantee steering.

5 Conclusion and discussion

In conclusion, we experimentally demonstrate the distribution of CV EPR entanglement in a 60.26 km fiber channel and CV quantum steering in a 10.06 km fiber channel by transmitting the EPR entangled lights and the LO light over independent fiber channels. In this case, the fiber-induced excess noise is reduced, enabling an extension of the transmission distance. By reconstructing the covariance matrices of distributed modes, we quantified the distributed CV EPR entanglement and steering through fiber channels. Our result takes a crucial step toward practical quantum communication with entanglement. Based on distributed quantum entanglement and steering, various quantum communication protocols can be achieved, such as quantum dense coding, quantum swapping, quantum secret sharing, quantum conference, and 1SDI quantum communication. Furthermore, the distributed entanglement and steering can be used to construct quantum communication networks.

In our experiment, the signal and the LO beams are transmitted through separate optical fibers to reduce the excess noise in fiber channels, which also introduces a challenge in maintaining stable phase locking between the two paths to minimize their relative phase fluctuations. Future efforts to enhance system stability and extend transmission distances could employ advanced strategies, such as optimized phase-locking systems, low-loss fibers, and a higher squeezing level of the CV entanglement source. Furthermore, the current distribution schemes for CV EPR entanglement and steering can be extended to multipartite quantum systems, including CV multipartite Greenberger-Horne-Zeilinger entangled systems and multipartite cluster entangled systems. So far, the proof-of-principle experiments of deterministic distribution of multipartite Gaussian entanglement and steering in a network with a quantum server and multiple users have been demonstrated [43,44]. Based on our research, a local quantum network involving quantum entanglement can be established by means of sharing a multipartite entangled state across quantum nodes over tens of kilometers of fiber channels. Such an extension would establish a versatile platform for practical multi-node quantum network applications.

Acknowledgements This work was supported by Innovation Program for Quantum Science and Technology (Grant No. 2024ZD0302403), National Natural Science Foundation of China (Grant Nos. 12434015, U25A20525, 62275145), and Fund for Shanxi '1331 Project' Key Subjects Construction.

Supporting information Appendixes A–C. The supporting information is available online at info.scichina.com and link.springer.com. The supporting materials are published as submitted, without typesetting or editing. The responsibility for scientific accuracy and content remains entirely with the authors.

References

1 Asavanant W, Furusawa A. Multipartite continuous-variable optical quantum entanglement: generation and application. Phys Rev A, 2024, 109: 040101
2 Du P, Zhang J, Zhang T, et al. A complete continuous-variable quantum computation architecture based on the 2D spatiotemporal cluster state. Sci Rep, 2025, 15: 18199
3 Pfister O. Continuous-variable quantum computing in the quantum optical frequency comb. J Phys B-At Mol Opt Phys, 2020, 53: 012001
4 Lloyd S, Braunstein S L. Quantum computation over continuous variables. Phys Rev Lett, 1999, 82: 1784–1787
5 Zhao S H, Tian W H, Liang X L, et al. Transport properties of $Tl_2Ba_2CaCu_2O_8$ microbridges on a low-angle step substrate. Chin Phys B, 2021, 30: 060308
6 Horodecki R, Horodecki P, Horodecki M, et al. Quantum entanglement. Rev Mod Phys, 2009, 81: 865–942
7 Zhang Y, Bian Y, Li Z, et al. Continuous-variable quantum key distribution system: past, present, and future. Appl Phys Rev, 2024, 11: 011318
8 Mizuno J, Wakui K, Furusawa A, et al. Experimental demonstration of entanglement-assisted coding using a two-mode squeezed vacuum state. Phys Rev A, 2004, 71: 012304
9 Li X, Pan Q, Jing J, et al. Quantum dense coding exploiting a bright Einstein-Podolsky-Rosen beam. Phys Rev Lett, 2002, 88: 047904
10 Jing J, Zhang J, Yan Y, et al. Experimental demonstration of tripartite entanglement and controlled dense coding for continuous variables. Phys Rev Lett, 2003, 90: 167903
11 Zhang J, Li Y, Zhao M, et al. One-sided device-independent random number generation through fiber channels. Light Sci Appl, 2025, 14: 25
12 Ren S Y, Han D M, Wang M H, et al. Continuous variable quantum teleportation and remote state preparation between two space-separated local networks. Sci China Inf Sci, 2024, 67: 142502
13 Wang N, Wang M, Ma C, et al. Controllable deterministic quantum teleportation of multiple sideband qumodes. Sci Bull, 2026, 71: 745–751
14 Ast M, Steinlechner S, Schnabel R. Reduction of classical measurement noise via quantum-dense metrology. Phys Rev Lett, 2016, 117: 180801
15 Fadel M, Roux N, Gessner M. Quantum metrology with a continuous-variable system. Rep Prog Phys, 2025, 88: 106001
16 Steinlechner S, Bauchrowitz J, Meinders M, et al. Quantum-dense metrology. Nat Photon, 2013, 7: 626–630
17 Einstein A, Podolsky B, Rosen N. Can the quantum-mechanical description of physical reality be considered complete? Phys Rev, 1935, 47: 696–702
18 Chang K C, Sarihan M C, Erker P, et al. Experimental high-dimensional entanglement certification and quantum steering with time-energy measurements. 2023. arXiv: 2310.20694
19 Chang K C, Sarihan M C, Cheng X, et al. Large-alphabet time-bin quantum key distribution and Einstein-Podolsky-Rosen steering via dispersive optics. Quantum Sci Technol, 2024, 9: 015018
20 Gallego R, Aolita L. Resource theory of steering. Phys Rev X, 2015, 5: 041008
21 Tomamichel M, Renner R. Uncertainty relation for smooth entropies. Phys Rev Lett, 2011, 106: 110506
22 Branciard C, Cavalcanti E G, Walborn S P, et al. One-sided device-independent quantum key distribution: security, feasibility, and the connection with steering. Phys Rev A, 2012, 85: 010301
23 Walk N, Hosseini S, Geng J, et al. Experimental demonstration of Gaussian protocols for one-sided device-independent quantum key distribution. Optica, 2016, 3: 634
24 Gehring T, Händchen V, Duhme J, et al. Implementation of continuous-variable quantum key distribution with composable and one-sided-device-independent security against coherent attacks. Nat Commun, 2015, 6: 8795
25 Cao W F, Zhen Y Z, Zheng Y L, et al. One-sided measurement-device-independent quantum key distribution. Phys Rev A, 2018, 97: 012313
26 Händchen V, Eberle T, Steinlechner S, et al. Observation of one-way Einstein-Podolsky-Rosen steering. Nat Photon, 2012, 6: 596–599
27 Qin Z, Deng X, Tian C, et al. Manipulating the direction of Einstein-Podolsky-Rosen steering. Phys Rev A, 2017, 95: 052114
28 Cavalcanti D, Skrzypczyk P, Aguilar G H, et al. Detection of entanglement in asymmetric quantum networks and multipartite quantum steering. Nat Commun, 2015, 6: 7941
29 Wollmann S, Walk N, Bennet A J, et al. Observation of one-way Einstein-Podolsky-Rosen steering. Phys Rev Lett, 2016, 116: 160403
30 Sun K, Ye X J, Xu J S, et al. Experimental quantification of asymmetric Einstein-Podolsky-Rosen steering. Phys Rev Lett, 2016, 116: 160404
31 Piani M, Watrous J. Necessary and sufficient quantum information characterization of Einstein-Podolsky-Rosen steering. Phys Rev Lett, 2015, 114: 060404
32 He Q, Rosales-Zárate L, Adesso G, et al. Secure continuous variable teleportation and Einstein-Podolsky-Rosen steering. Phys Rev Lett, 2015, 115: 180502
33 Liu S, Han D, Wang N, et al. Experimental demonstration of remotely creating Wigner negativity via quantum steering. Phys Rev Lett, 2022, 128: 200401
34 Ren S, Yan Y, Li Y, et al. Deterministic entanglement-assisted quantum communication over 20 km fiber channel. Light Sci Appl, 2026, 15: 83
35 Achatz L, Bulla L, Ecker S, et al. Simultaneous transmission of hyper-entanglement in three degrees of freedom through a multicore fiber. npj Quantum Inf, 2023, 9: 45
36 Joseph Marcellino F, Caspar P, Brydges T, et al. Toward heralded distribution of polarization entanglement. Optica Quantum, 2024, 2: 181
37 Li C, Ren S Y, Yan Y R, et al. Distribution of polarization squeezed light through a 20 km fiber channel. Sci China Inf Sci, 2024, 67: 159501
38 Feng J, Wan Z, Li Y, et al. Distribution of continuous variable quantum entanglement at a telecommunication wavelength over 20 km of optical fiber. Opt Lett, 2017, 42: 3399
39 Deng X, Liu Y, Wang M, et al. Sudden death and revival of Gaussian Einstein-Podolsky-Rosen steering in noisy channels. npj Quantum Inf, 2021, 7: 65
40 Garcia-Chung A. On the covariance matrix for Gaussian states. 2020. arXiv: 2003.11063
41 Simon R. Peres-Horodecki separability criterion for continuous variable systems. Phys Rev Lett, 2000, 84: 2726–2729
42 Kogias I, Lee A R, Ragy S, et al. Quantification of Gaussian quantum steering. Phys Rev Lett, 2015, 114: 060403
43 Wang M, Xiang Y, Kang H, et al. Deterministic distribution of multipartite entanglement and steering in a quantum network by separable states. Phys Rev Lett, 2020, 125: 260506
44 Yonezawa H, Aoki T, Furusawa A. Demonstration of a quantum teleportation network for continuous variables. Nature, 2004, 431: 430–433